The Heterocyclic Diradical Benzo-1,2:4,5-bis(1,3,2-dithiazolyl). Electronic, Molecular and Solid State Structure

T. M. Barclay,[1a] A. W. Cordes,[1a] R. H. de Laat,[1b] J. D. Goddard,[1b] R. C. Haddon,[1c] D. Y. Jeter,[1a] R. C. Mawhinney,[1b] R. T. Oakley,*[,1b] T. T. M. Palstra,[1c] G. W. Patenaude,[1b] R. W. Reed,[1b] and N. P. C. Westwood[1b]

Contribution from the Department of Chemistry and Biochemistry, University of Arkansas, Fayetteville, Arkansas 72701, Department of Chemistry and Biochemistry, University of Guelph, Guelph, Ontario, N1G 2W1 Canada, and Bell Laboratories, Lucent Technologies, 600 Mountain Avenue, Murray Hill, New Jersey 07974

Received October 17, 1996[⊗]

Abstract: The preparation and purification of the heterocyclic diradical benzo-1,2:4,5-bis(1,3,2-dithiazolyl) (BBDTA) is described. Crystals of BBDTA, grown by fractional sublimation at 120−180 °C/10^{-3} Torr, are monoclinic, space group $P2_1/c$, with $a = 4.144(2)$, $b = 9.0344(13)$, and $c = 10.7424(16)$ Å, $\beta = 91.11(3)°$, and $Z = 2$. The crystal structure consists of discrete, unassociated molecules of BBDTA. The molecules form slipped stacks along the *x* direction, with the mean molecular plane making an angle of 32.4° to the *x* axis. The interplanar separation between consecutive molecules along the stacking direction is 3.49 Å. The ESR spectrum of BBDTA is solvent dependent, displaying signals attributable to partially associated materials (*not* exchange coupled) and to free diradical (exchange coupled). *Ab initio* molecular orbital calculations suggest a small (*ca*. 0.5 kcal/mol) separation between the triplet and singlet diradical states. Cyclic voltammetry on BBDTA and the related benzo-1,3,2-dithiazolyl BDTA, coupled with gas phase photoelectron studies on BDTA, establish that both compounds are strong electron donors. Magnetic susceptibility measurements show that BBDTA is essentially diamagnetic up to room temperature; variable temperature single-crystal conductivity measurements provide a band gap of 0.22 eV. The transport properties are discussed in the light of extended Hückel band structure calculations, which suggest a highly three-dimensional electronic structure for bulk BBDTA in the solid state.

Introduction

The last decade has seen an increasing interest in the synthesis and solid state properties of neutral heterocyclic π-radicals.[2] Most of our work in this area has focused on derivatives of the 1,2,3,5-dithiadiazolyl system **1** and their selenium counterparts,[3] with the intent of using these materials as building blocks for molecular conductors.[4] To this end we have prepared a wide range of diradical[5] and triradical[6] derivatives, *e.g.*, the "back-to-back" diradical **2**[7] and the 1,4-benzene-bridged compound **3**.[5a] The conductivity of these materials is generally low, but doping with halogens can lead to dramatic improvements; several iodine charge transfer salts exhibiting metallic behavior at room temperature have been described.[7,8]

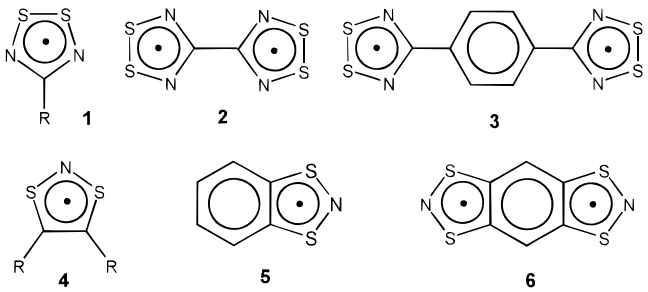

Another heterocyclic sulfur−nitrogen radical which holds promise as a building block for molecular materials is the 1,3,2-dithiazolyl or DTA system (**4**). A variety of monofunctional radicals have been observed by ESR spectroscopy.[9,10] Some, including the benzo derivative BDTA **5**, have been isolated[11] and characterized in the solid state by X-ray crystallography.[12−15] The diradical benzo-1,2:4,5-bis(1,3,2-dithiazolyl) (BBDTA, **6**)

[⊗] Abstract published in *Advance ACS Abstracts,* February 15, 1997.

(1) (a) University of Arkansas. (b) University of Guelph. (c) AT&T Bell Laboratories.

(2) (a) Banister, A. J.; Rawson, J. M. In *The Chemistry of Inorganic Ring Systems*; Steudel, R., Ed.; Elsevier: Amsterdam, 1992; p 323. (b) Banister, A. J.; Rawson, J. M. *Adv. Heteroat. Chem.* **1995**, *62*, 137. (c) Oakley, R. T. *Prog. Inorg. Chem.* **1988**, *36*, 299.

(3) (a) Cordes, A. W.; Haddon, R. C.; Oakley, R. T. In *The Chemistry of Inorganic Ring Systems*; Steudel, R., Ed.; Elsevier: Amsterdam, 1992; p 295. (b) Cordes, A. W.; Haddon, R. C.; Oakley, R. T. *Adv. Mater*. **1994**, *6*, 798.

(4) (a) Haddon, R. C. *Nature (London)* **1975**, *256*, 394. (b) Haddon, R. C. *Aust. J. Chem.* **1975**, *28*, 2343.

(5) (a) Cordes, A. W.; Haddon, R. C.; Oakley, R. T.; Schneemeyer, L. F.; Waszczak, J. V.; Young, K. M.; Zimmerman, N. M. *J. Am. Chem. Soc.* **1991**, *113*, 582. (b) Andrews, M. P.; Cordes, A. W.; Douglass, D. C.; Fleming, R. M.; Glarum, S. H.; Haddon, R. C.; Marsh, P.; Oakley, R. T.; Palstra, T. T. M.; Schneemeyer, L. F.; Trucks, G. W.; Tycko, R.; Waszczak, J. V.; Young, K. M.;Zimmerman, N. M. *J. Am. Chem. Soc.* **1991**, *113*, 3559.

(6) (a) Cordes, A. W.; Haddon, R. C.; Hicks, R. G.; Oakley, R. T.; Palstra, T. T. M.; Schneemeyer, L. F.; Waszczak, J. V. *J. Am. Chem. Soc*. **1992**, *114*, 5000. (b) Cordes, A. W.; Haddon, R. C.; Hicks, R. G.; Kennepohl, D. K.; Oakley, R. T.; Schneemeyer, L. F.; Waszczak, J. V. *Inorg. Chem.* **1993**, *32*, 1554.

(7) (a) Bryan, C. D.; Cordes, A. W.; Goddard, J. D.; Haddon, R. C.; Hicks, R. G.; Oakley, R. T.; Palstra, T. T. M.; Perel, A. S. *J. Chem. Soc., Chem. Commun*. **1994**, 1447. (b) Bryan, C. D.; Cordes, A. W.; Goddard, J. D.; Haddon, R. C.; Hicks, R. G.; Mackinnon, C. D.; Mawhinney, R. C.; Oakley, R. T.; Palstra, T. T. M.; Perel, A. S. *J. Am. Chem. Soc*. **1996**, *118*, 330.

(8) (a) Bryan, C. D.; Cordes, A. W.; Haddon, R. C.; Glarum, S. H.; Hicks, S. H.; Kennepohl, D. K.; MacKinnon, C. D.; Oakley, R. T.; Palstra, T. T. M.; Perel, A. S.; Schneemeyer, L. F.; Scott, S. R.; Waszczak, J. V. *J. Am. Chem. Soc*. **1994**, *116*, 1205. (b) Bryan, C. D.; Cordes, A. W.; Fleming, R. M.; George, N. A.; Glarum, S. H.; Haddon, R. C.; MacKinnon, C. D.; Oakley, R. T.; Palstra, T. T. M.; Perel, A. S. *J. Am. Chem. Soc*. **1995**, *117*, 6880. (c) Bryan, C. D.; Cordes, A. W.; George, N. A.; Haddon, R. C.; MacKinnon, C. D.; Oakley, R. T.; Palstra, T. T. M.; Perel, A. S. *Chem. Mater*. **1996**, *8*, 762.

S0002-7863(96)03629-3 CCC: $14.00

Scheme 1

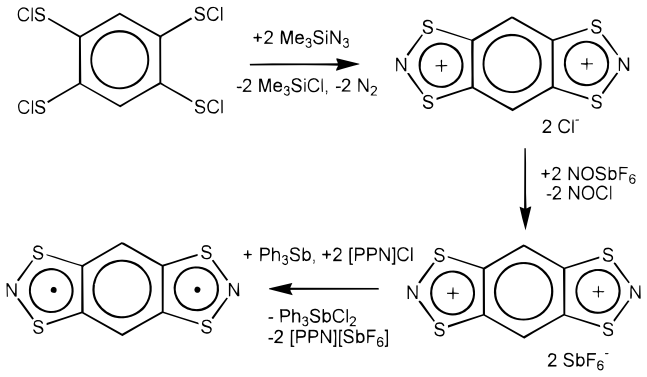

has also been pursued by several research groups, but characterization of this species is incomplete.[16,17] Both the diradical and its radical cation have been identified by ESR spectroscopy, and a salt containing the dimerized radical cation has also been reported.[18] However, neither the structure of the diradical nor its solid state transport properties have ever been determined. As a key step in establishing the potential of dithiazolyl radicals in molecular conductor design, we have performed a comprehensive synthetic and structural investigation of BBDTA itself; herein, we report its isolation, purification, and solid state characterization. The electronic structures of BBDTA (**6**, isolated molecule) and the related dithiazolyls DTA (**4**, R = H) and BDTA (**5**) have been examined by *ab initio* molecular orbital methods. These computational results, coupled with cyclic voltammetry on both BDTA and BBDTA and photoelectron spectroscopic studies on BDTA, provide a clear picture of the electronic and redox behavior of these molecules. Variable temperature magnetic susceptibility and conductivity measurements on solid BBDTA have also been performed, and the results have been interpreted in the light of extended Hückel band calculations.

Results and Discussion

Synthesis. The preparation (Scheme 1) of the skeletal framework of BBDTA builds from the synthetic sequence developed by Wolmershäuser[16] and by Wudl.[17] In this work, however, several important procedural changes and/or purification steps were introduced. For example, benzene-1,2,4,5-tetra(sulfenyl chloride), prepared by oxidation of the corresponding tetrathiol, was here crystallized from carbon tetrachloride before condensation with 2 equiv of trimethylsilyl azide in methylene chloride. The dark red dichloride $[BBDTA]Cl_2$ so obtained was then converted by metathesis with nitrosyl hexafluoroantimonate into the corresponding bis(hexafluorantimonate) salt $[BBDTA][SbF_6]_2$, which was recrystallized from chlorobenzene/acetonitrile. Reduction of the purified salt to neutral BBDTA could be effected, on a milligram scale, by electrolysis from an acetonitrile solution at 50 μA onto a Pt wire cathode. Larger quantities could be obtained by chemical reduction, but this approach required very specific conditions. Attempts to reduce $[BBDTA][SbF_6]_2$ directly with silver or zinc powder in acetonitrile afforded a black solid and a dark blue solution. While very small quantities of impure BBDTA could be recovered from the solution, the black material proved to be totally intractable (its IR spectrum indicated that BBDTA was not present). The most successful approach involved the use of triphenylantimony as reducing agent, plus bis(triphenylphosphine)iminium chloride (PPNCl) as a chloride ion source. Under these conditions, a microcrystalline precipitate of BBDTA was produced. The crude product was purified by fractional sublimation in a gradient tube furnace at 120−80 °C/10^{-3} Torr to afford lustrous copper-colored blocks. In the solid state, BBDTA appears to be indefinitely stable in air. It is soluble in organic media (CH_2Cl_2, CH_3CN) to a level of *ca.* 5 mg L^{-1} to give deep blue solutions which are remarkably stable toward atmospheric oxygen.

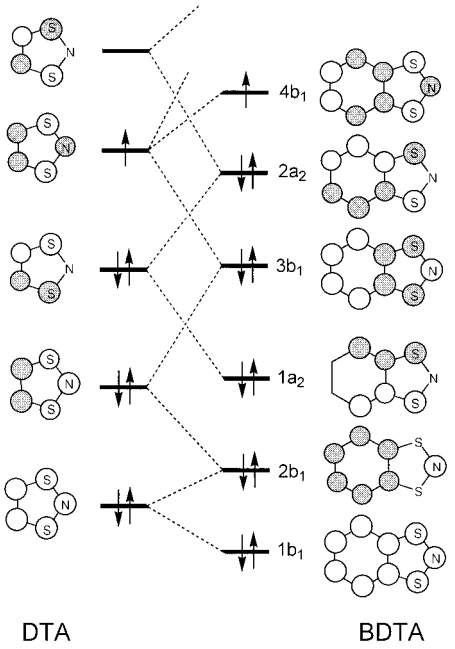

Figure 1. Qualitative MO energy level diagram illustrating the evolution of the 7π-manifold of DTA (left) to the 11π-manifold of BDTA (right). Orbital energies are approximate but are ordered according to the *ab initio* results.

Electronic Structure of BBDTA. As a first step in examining the chemical and physical properties of BBDTA, we have performed a series of *ab initio* molecular orbital calculations on BBDTA itself and several smaller, related monoradicals, namely the prototypal DTA radical **4** (R = H)[9b] and the benzo derivative BDTA (**5**).[13] Figure 1 provides a qualitative molecular orbital energy level diagram for the 7 π-electron radical DTA (**4**, R = H) and illustrates the correlation of these orbitals with the corresponding π-manifold of the 11 π-electron benzo

(9) (a) Preston, K. F.; Sutcliffe, L. H. *Magn. Reson. Chem.* **1990**, *28*, 189. (b) Chung, Y.-L.; Fairhurst, S. A.; Gillies, D. G.; Preston, K. F.; Sutcliffe, L. H. *Magn. Reson. Chem.* **1992**, *30*, 666.

(10) (a) Awere, E. G.; Burford, N.; Mailer, C.; Passmore, J.; Schriver, M. J.; White, P. S.; Banister, A. J.; Oberhammer, H.; Sutcliffe, L. J. *J. Chem. Soc., Chem. Commun.* **1987**, 66. (b) MacLean, G. K.; Passmore, J.; Rao, M. N. S.; Schriver, M. J.; White, P. S. *J. Chem. Soc., Dalton Trans.* **1985**, 1405. (c) Wolmershäuser, G.; Kraft, G. *Chem. Ber.* **1989**, *122*, 385. (d) Harrison, S. R.; Pilkington, R. S.; Sutcliffe, L. H. *J. Chem. Soc., Faraday Trans. 1* **1984**, *80*, 669. (e) Fairhurst, S. A.; Pilkington, R. S.; Sutcliffe, L. H. *J. Chem. Soc., Faraday Trans. 1* **1983**, *79*, 439. (f) Fairhurst, S. A.; Pilkington, R. S.; Sutcliffe, L. H. *J. Chem. Soc., Faraday Trans. 1* **1983**, *79*, 925. (g) Chung, Y.-L.; Sandall, J. P. B.; Sutcliffe, L. H.; Joly, H.; Preston, K. F.; Johann, R.; Kraft, G.; Wolmershäuser, G. *Magn. Reson. Chem.* **1991**, *29*, 625.

(11) Wolmershäuser, G.; Schnauber, M.; Willhelm, T. *J. Chem. Soc., Chem. Commun.* **1984**, 573.

(12) Wolmershäuser, G.; Kraft, G. *Chem. Ber.* **1990**, *123*, 881.

(13) Awere, E. G.; Burford, N.; Haddon, R. C.; Parsons, S.; Passmore, J.; Waszczak, J. V.; White, P. S. *Inorg. Chem.* **1990**, *29*, 4821.

(14) Wolmershäuser, G.; Johann, R. *Angew. Chem., Int. Ed. Engl.* **1989**, *28*, 920.

(15) Heckmann, G.; Johann, R.; Kraft, G.; Wolmershäuser, G. *Synth. Met.* **1991**, *41*−*43*, 3287.

(16) Wolmershäuser, G.; Schnauber, W.; Wilhelm, T.; Sutcliffe, L. H. *Synth. Met.* **1986**, *14*, 233.

(17) (a) Williams, K. A.; Nowak, M. J.; Dormann, E.; Wudl, F. *Synth. Met.* **1986**, *14*, 233. (b) Dormann, E.; Nowak, M. J.; Williams, K. A.; Angus, R. O., Jr.; Wudl, F. *J. Am. Chem. Soc.* **1987**, *109*, 2594.

(18) Wolmershäuser, G.; Wortmann, G.; Schnauber, M. *J. Chem. Res., Synop.* **1988**, 358.

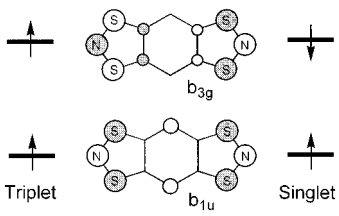

Figure 2. Singly occupied orbitals b_{1u} and b_{3g} of BBDTA and schematic representations of the singlet diradical and triplet configurations arising therefrom. (The molecule lies in the *xy* plane, with +*y* to the right.)

derivative. These correlations, which will be used later to interpret the photoelectron spectrum of BDTA, illustrate the strong mixing that occurs between the b_1 singly occupied molecular orbital (SOMO) of DTA with the π-system of benzene.

This SOMO mixing with benzene also occurs in BBDTA, but now there are two radical centers, and the extent of intramolecular exchange interactions between the two unpaired spins is a primary concern. Indeed, early work on BBDTA was prompted by its potential in the design of organic ferromagnets,[17] for which a high-spin ground state was desired. In our recent study of the "back-to-back" diradical **2**,[7] we concluded that exchange coupling was very small; the energies of the triplet and open shell singlets were within 1 kcal/mol. That system represented a classic example of a disjoint diradical, *i.e.*, one in which the molecular orbitals for the two unpaired electrons can be localized identically onto two separate groups of atoms.[19,20] The BBDTA system, however, is not formally disjoint, as the in-phase and out-of-phase combinations of radical SOMOs mix, to different extents, with orbitals of the bridging benzene ring. Thus, even at the Hückel level, the resulting b_{1u} and b_{3g} combinations (Figure 2) are not degenerate. In order to probe the energetic differences between the triplet $^3B_{2u}$ and diradical singlet $^1B_{2u}$ states that arise from this configuration,[21] we have performed calculations with a cep-31+g** basis set at both the Hartree−Fock and single-point CI level. These show that despite the formal nondegeneracy of the b_{1u} and b_{3g} orbitals, the two spin states are remarkably close in energy, with the singlet lying slightly (*ca*. 0.5 kcal/mol) above the triplet.

The second issue which deserves examination is the energetics of charge transfer to and from DTA, BDTA, and BBDTA. From the perspective of molecular conductor design, these conversions are of particular relevance, as the difference between the ionization potential (IP) and electron affinity (EA), the disproportionation energy (IP − EA), provides a measure of the Coulombic barrier to charge transfer between adjacent sites in the solid state. Table 1 summarizes the calculated (ΔSCF, cep-31+g**) values of the IP and EA for DTA, BDTA, and BBDTA.[22] The IP values are remarkably similar for the three compounds and establish the DTA system as being significantly more electron-rich than other sulfur−nitrogen heterocyclic radicals, *e.g.*, 1,2,3,5-dithiadiazolyls and 1,2,4,6-thiatriazinyls, all of which exhibit IP values between 7 and 9 eV.[23] Also of note is the increase in EA along the series DTA, BDTA, and BBDTA, which we interpret as a manifestation of the ability of the larger molecules to redistribute charge more effectively. Largely as a result of these changes in EA, the value of the disproportionation energy (IP − EA) in BDTA and BBDTA is smaller than in DTA. Also provided in Table 1 are the calculated bond lengths within the heterocyclic framework as a function of oxidation state. Table 2 provides a summary of the corresponding charge distributions. All geometries were optimized without symmetry constraints, and full vibrational analyses confirm that these structures are energy minima. The final geometries of the cations and radicals were essentially planar, with symmetries very close to C_{2v} (DTA, BDTA) and

Table 1. Predicted[a] (ΔSCF) Adiabatic IP Values (eV), EA Values (eV), and Disproportionation Energies (IP − EA) of DTA (**4**, R = H), BDTA, and BBDTA and Optimized Bond Distances (in Å) of the Neutral Species and Corresponding Cations and Anions

	DTA^+	$BDTA^+$	$BBDTA^+$
S−N	1.589	1.588	1.652
C−S	1.704	1.726	1.729
C−C	1.375	1.412	1.446
	DTA	BDTA	BBDTA[b]
S−N	1.677	1.681	1.670
C−S	1.763	1.774	1.765
C−C	1.341	1.399	1.411
IP	6.59	6.54	6.80
EA	−0.28	0.05	0.17
(IP − EA)	6.87	6.49	6.63
	DTA^- [c]	$BDTA^-$ [c]	$BBDTA^-$ [c]
S−N	1.725	1.724	1.679/1.722[d]
	(1.763)	(1.749)	(1.688)
C−S	1.790	1.785	1.776/1.782[d]
	(1.773)	(1.768)	(1.747)
C−C	1.346	1.419	1.389/1.429[d]
	(1.346)	(1.423)	(1.426)

[a] cep-31+g** basis set; all geometries fully optimized unless otherwise indicated. [b] Predictions on neutral BBDTA are for the triplet ($^3B_{2u}$) state. [c] The numbers in parentheses refer to calculations (cep-31g**) in which planarity has been enforced. [d] The first number refers to the formally neutral ring, the second to the formally reduced ring.

Table 2. Predicted[a] Mulliken Net Atomic Charges in DTA (**4**, R = H), BDTA, and BBDTA and the Corresponding Cations and Anions

	DTA^+	$BDTA^+$	$BBDTA^+$
q_N	−0.198	−0.170	−0.216
q_S	0.414	0.361	0.259
q_C	−0.082	−0.173	−0.168
	DTA	BDTA	BBDTA[b]
q_N	−0.314	−0.288	−0.283
q_S	0.112	0.095	0.119
q_C	−0.163	−0.145	−0.196
	DTA^- [c]	$BDTA^-$ [c]	$BBDTA^-$ [c]
q_N	−0.663	−0.648	−0.319, −0.638[d]
	(−0.697)	(−0.668)	(−0.563)
q_S	−0.101	−0.090	0.046, −0.058[d]
	(−0.098)	(−.094)	(0.005)
q_C	−0.225	−0.159	−0.192, −0.210[d]
	(−0.206)	(−0.114)	(−0.171)

[a] cep-31g** basis set; all geometries fully optimized unless otherwise indicated. [b] Predictions on neutral BBDTA refer to the triplet ($^3B_{2u}$) state. [c] The numbers in parentheses refer to calculations in which planarity has been enforced. [d] The first number refers to the formally neutral ring, the second to the formally reduced ring.

(19) (a) Borden, W. T.; Davidson, E. R. *J. Am. Chem. Soc.* **1977**, *99*, 4587. (b) Pranata, J. *J. Am. Chem. Soc.* **1992**, *114*, 10537. (c) Racja, A. *Chem. Rev.* **1994**, *94*, 871.

(20) (a) Borden, W. T. In *Diradicals*; Borden, W. T., Ed.; J. Wiley and Sons: New York, 1982; p 24. (b) Salem, L. *Electrons in Chemical Reactions: First Principles*; Wiley Interscience: Chichester, U.K., 1982; Chapter 3. (c) Salem, L.; Rowland, C. *Angew. Chem., Int. Ed. Engl.* **1972**, *11*, 92.

(21) There are also two other closed shell zwitterionic singlet states. Both of these are much higher lying than those described here.

(22) For BBDTA, the IP and EA values are calculated with reference to the triplet ($^3B_{2u}$) state.

(23) (a) Boeré, R. T.; Oakley, R. T.; Reed, R. W.; Westwood, N. P. C. *J. Am. Chem. Soc.* **1989**, *111*, 1180. (b) Cordes, A. W.; Goddard, J. D.; Oakley, R. T.; Westwood, N. P. C. *J. Am. Chem. Soc.* **1989**, *111*, 6147. (c) Bryan, C. D.; Cordes, A. W.; Haddon, R. C.; Hicks, R. G.; Kennepohl, D. K.; MacKinnon, C. D.; Oakley, R. T.; Palstra, T. T. M.; Perel, A. S.; Scott, S. R.; Schneemeyer, L. F.; Waszczak, J. V. *J. Am. Chem. Soc.* **1994**, *116*, 1205.

D_{2h} (BBDTA). The symmetric charge distribution in $BBDTA^+$, which is reflected in its ESR spectrum,[16,17] indicates that charge depletion from the two C_2S_2N rings in $BBDTA^+$ relative to those in BBDTA is *ca*. 50% of that found upon oxidation of either of the two monofunctional radicals. In all cases sulfur is the largest source of charge for the oxidation process.

In contrast to the planar geometries found for the higher oxidation states, the minimum energy structures for DTA^- and $BDTA^-$ have C_s symmetry with the plane of the SNS unit folding, in an envelope-like fashion, away from the plane of the other atoms by *ca*. 26°. Although there are no known structures of anionic derivatives, this ring puckering has been observed experimentally, *e.g*., in the covalent toluenesulfonamide derivative **7**, where the fold angle is 41.7°.[24] Calculations

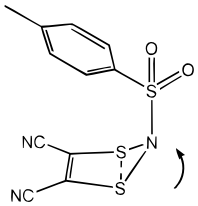

7

on DTA^- and $BDTA^-$ in which planarity was enforced reveal that the planar geometry, which can be loosely related to the transition state of the ring inversion process lies, respectively, 7.2 and 7.8 kcal/mol above the puckered form. This tendency to pucker into an envelope shape is also predicted in $BBDTA^-$, where the negative charge is localized heavily on one C_2S_2N ring. The charge distribution in the other C_2S_2N ring resembles that found in a neutral radical. However, a calculation on $BBDTA^-$ in which planarity was enforced reveals a very different charge distribution. With this symmetry constraint in place the symmetry of the charge distribution is essentially D_{2h}, *i.e*., the negative charge is evenly distributed over the two heterocyclic rings. The shift of electron density only occurs when the restriction to planarity is removed. As a result of the major electronic reorganization associated with the puckering process, the energy difference between planar and nonplanar forms of $BBDTA^-$ is substantially larger (23.3 kcal/mol) than that found for DTA^- and $BDTA^-$.

The structural parameters of all three compounds show similar trends as a function of oxidation state; the S−N and S−C bonds lengthen with progressive reduction from cation to radical to anion. These changes can be understood within the confines of the molecular orbital arguments already well developed.[13] For example, in DTA the b_1 SOMO (Figure 1) is antibonding over the S−N and S−C bonds; oxidation of DTA leads to shortening of these linkages, while its reduction caused them to lengthen. In the radical cation $BBDTA^+$, the singly occupied orbital (b_{1u} in Figure 2) is delocalized over both dithiazole rings, so that the S−N and S−C bond lengths are intermediate between those found in neutral and fully oxidized rings, *i.e*., DTA^+ and $BDTA^+$. In the fully optimized (C_s) version of $BBDTA^-$, the structural parameters of the two C_2S_2N rings resemble those expected for one isolated anion and one isolated radical. In the model planar structure, in which the additional electron is delocalized over the entire molecule, the S−N and (to a lesser extent) the S−C bonds in the two heterocyclic rings are essentially equal, with values that are approximately intermediate between those expected for a neutral radical and those expected for a fully reduced anion.

Crystal Structure. To date several monofunctional dithiazolyl radicals have been characterized by X-ray crystallography.

(24) Wolmershäuser, G.; Kraft, G. *Chem. Ber*. **1989**, *122*, 385.

Table 3. Atomic Parameters *x*, *y*, *z* and B_{eq}/B_{iso}[a]

	x	*y*	*z*	B_{eq}/B_{iso}[b]
S1	0.60625(16)	0.09088(7)	0.23082(6)	3.13(3)
S2	0.75079(17)	0.31438(7)	0.06578(6)	3.29(3)
N	0.5730(6)	0.2678(2)	0.1960(2)	3.49(9)
C1	0.9206(6)	−0.1157(2)	0.0836(2)	2.57(9)
C2	0.8226(5)	0.0294(3)	0.1049(2)	2.41(9)
C3	0.9007(6)	0.1432(3)	0.0216(2)	2.36(9)
H	0.870	−0.193	0.140	3.4

[a] ESDs refer to the last digit printed. [b] B_{eq} is the mean of the principal axes of the thermal ellipsoid.

The 4,5-dicyano derivative associates to form the cofacial dimer **8**,[12] while the benzo derivative BDTA dimerizes in the centrosymmetric manner (**9**).[13] The mean interannular S···S distances in these dimers are 3.145 and 3.175 Å, respectively. Cofacial dimerization is also observed for the pyrazine derivative **10**, but in this case the dimers form one-dimensional stacks.[15] These observations, *i.e*., of spin-paired dimers, are reminiscent of the solid state features of 1,2,3,5-dithiadiazolyls **1**, which almost invariably crystallize as closed shell dimers (except when inhibited by steric bulk[25]). Association is also found in the salt [BBDTA][$FeCl_4$], which consists of the dimeric dication **11**.[18] However, there is one reported instance, involving the trithiatriazapentalenyl system (TTP) **12**, of a dithiazolyl that does not associate in the solid state.[14] In this structure the absence of association cannot be attributed to steric effects. The structure of BBDTA also falls into this latter category.

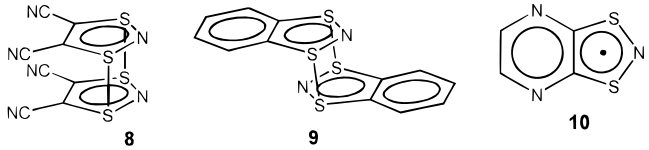

8

9

10

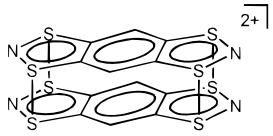

11

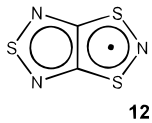

12

Crystals of BBDTA grown by vacuum sublimation belong to the monoclinic space group $P2_1/c$; atomic coordinates are provided in Table 3. The structure consists of discrete (undimerized) BBDTA molecules which lie on a center of inversion; the molecules are planar with the largest deviation from the mean plane being 0.014(3) Å (for C3). The intramolecular bond distances[26] are all in close agreement with those predicted by the *ab initio* calculations. The packing of BBDTA molecules, as viewed down the *x* direction, is illustrated in Figure 3A. The interlocking nature of this arrangement leads to numerous short intermolecular contacts; most notable are the two S···S contacts d_1 and d_2 and the S···N contact d_3. The molecules form strongly slipped stacks along the *x* direction (Figure 3B), with the mean molecular plane making an angle of 32.4° with the *x* axis. The mean interplanar separation between consecutive molecules along the stacking direction is 3.49 Å. It is interesting to note that the packing pattern of TTP

(25) (a) Banister, A. J.; Bricklebank, N.; Clegg, W.; Elsegood, M. R. J.; Gregory, C. I.; Lavender, I.; Rawson, J. M.; Tanner, B. K. *J. Chem. Soc., Chem. Commun*. **1995**, 679. (b) Banister, A. J.; Bricklebank, N.; Lavender, I.; Rawson, J. M.; Gregory, C. I.; Tanner, B. K.; Clegg, W.; Elsegood, M. R. J.; Palacio, F. *Angew. Chem., Int. Ed. Engl*. **1996**, *35*, 2533.

(26) Intramolecular structural parameters for BBDTA include the following: d(S1−N) = 1.647(2), d(S2−N) = 1.648(2), d(S1−C2) = 1.729(2), d(S2−C3) = 1.736(2), d(C1−C2) = 1.392(2), d(C2−C3) = 1.405(3), and d(C1−C3a) = 1.386(3) Å; S1−N−S2 = 113.81(12)°.

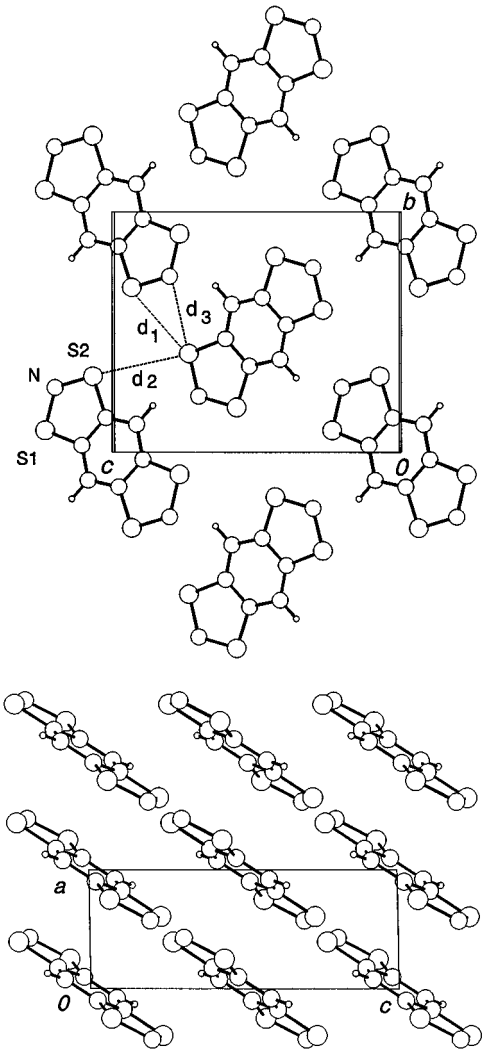

Figure 3. (A) Packing of BBDTA viewed down the *x* direction (above). Close intermolecular contacts are S1···S2′ (d_1) 3.651(1), S1···S2′ (d_2) 3.736(1), and S1···N′ (d_3) 3.116(2)Å. (B) Slipped stacks of BBDTA running parallel to the *x* direction (below).

(**12**) also consists of slipped stacks (cell repeat = 3.697 Å) with the mean molecular plane making an angle of 35.1° to the stacking direction.

As expected from the molecular orbital discussion and computed geometries provided above, the experimental S−N and S−C bond distances in BBDTA are very close to those observed in the neutral systems $[BDTA]_2$ (**9**) and TTP (**12**).[13,14] Oxidation of the diradical BBDTA to the radical cation $[BBDTA]^+$ (as found in the dimer dication **11**)[18] leads to a contraction in the skeletal S−N and S−C bonds to distances which are intermediate between those typically found in neutral materials and fully oxidized structures, *e.g.*, [BDTA]Cl[13] and [BDTA]I.[27]

ESR Spectrum. The ESR spectrum of BBDTA has been examined extensively by previous workers.[16,17] Our results concur with the earlier findings and also provide additional insight into the extent of association and exchange interactions between the two radical centers. As noted before, the ESR spectrum of BBDTA is both solvent and sample dependent. When BBDTA is dissolved in methylene chloride at room temperature, the ESR spectrum (Figure 4) is almost identical to that reported earlier, *i.e.*, a relatively well-resolved triplet of

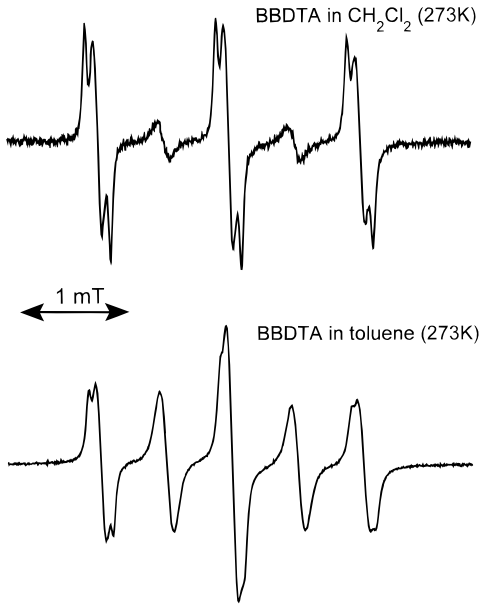

Figure 4. ESR spectrum of BBDTA in CH_2Cl_2 (above) and toluene (below) at 273 K.

triplets (*tot*) pattern with a_N = 11.3 mT, a_H = 0.68 mT, and g = 2.0067. These values are typical of simple 1,3,2-dithiazolyls[9] and indicate substantial spin density on nitrogen. Small additional signals are also observed midway between the main tot peaks, and the nature of these has been the subject of some debate. Isotope effects, exchange interactions and the possibility of two superimposed signals have been considered. We also note that, as reported earlier, the overall intensity of the ESR signal is weak, relative to the concentration of the sample. This suggests that the dominant species in solution is closed shell.

Association of the BBDTA diradical **6** can clearly occur in a variety of modes in solution. We conclude that the strong *tot* signals originate from a partially associated species such as **13** (*cf.*, the solid state structure **9**). In this species, the two radical centers are sufficiently removed from one another that the spectrum should resemble that expected for two separate and noninteracting spin doublets. Association could also occur to afford the diamagnetic dimer **14**, which would not exhibit any ESR signal. The broader, weak lines between the *tot* signals are a manifestation of an exchange-coupled species.[28,29] We assign these lines to free, unassociated BBDTA. This interpretation was supported by recording the spectrum in toluene (Figure 4, g = 2.0069). In this medium, solvation effects favor free BBDTA over the open-ended dimer **13**, and the appearance of the spectrum, *i.e.*, a broad pentet, is consistent with that expected for a single diradical for which exchange coupling (J_{ex}) is much greater than hyperfine coupling a_N. Other solvents (chlorobenzene, benzene) produce effects intermediate between the two extremes illustrated in Figure 4. Variations in the overall concentration of BBDTA also lead to small changes in the balance between signals for **13** (*tot*) and **6** (*pentet*). We have also recorded the frozen glass spectrum of BBDTA in a 2-methyltetrahydrofuran matrix at −120 °C; its appearance was virtually identical to that observed earlier by Wudl and co-workers.[17] We concur with their conclusion that the breadth of the spectrum, along with the absence of any half-field signal

(27) Oakley, R. T.; Spence, R. E. v. H.; Richardson, J. F. *Acta Crystallogr.* **1995**, *C51*, 1654.

(28) (a) Weil, J. A.; Bolton, J. R.; Wertz, J. E. In *Electron Paramagnetic Resonance*; John Wiley and Sons: New York, 1993; Section 6.4. (b) Glarum, S. H.; Marshall, J. H.; *J. Chem. Phys.* **1967**, *47*, 1374. (c) Brière, R.; Dupeyre, R. M.; Lemaire, H.; Morat, C.; Rassat, A.; Rey, P. *Bull. Soc. Chim. Fr.* **1965**, 3290.

(29) Bencini, A.; Gatteschi, D. In *EPR of Exchange Coupled Systems*; Springer-Verlag: New York, 1990; p 187.

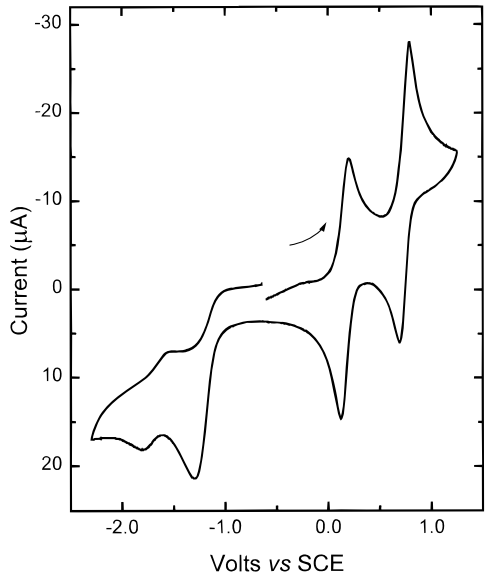

Figure 5. Cyclic voltammogram of BBDTA in CH_3CN (Pt wire, 0.1 M Bu_4NPF_6), scan rate 50 mV s^{-1}.

that could be attributed to a triplet ground state, provides additional support for the conclusion that the ESR spectrum arises from an associated species such as **13**.

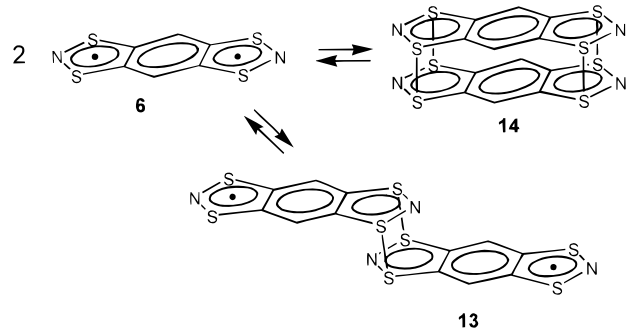

Cyclic Voltammetry and Photoelectron Spectroscopy. We have examined the redox behavior of both BDTA and BBDTA in solution by cyclic voltammetry (CV). Cyclic voltammetry (Figure 5) on a saturated solution of BBDTA in acetonitrile (Pt wire electrodes, 0.1 M Bu_4NPF_6 as supporting electrolyte, *vs* SCE) reveals two reversible oxidation waves with $E_{1/2}$ values of 0.16 V for the BBDTA/$BBDTA^+$ couple and 0.74 V for the $BBDTA^+$/$BBDTA^{2+}$ couple. In addition, two irreversible reduction waves with cathodic peak potentials (E_{pc}) of −1.3 and −1.8 V are also observed. Under similar conditions, cyclic voltammetry on BDTA reveals a single reversible oxidation wave at 0.15 V and an irreversible wave with $E_{pc} = -1.2$ V.

While the vapor pressure of BBDTA is prohibitively low, we have been able to record the gas phase HeI ultraviolet photoelectron (UPS) spectrum of BDTA and, thus, have been able to bridge together the solution-based electrochemical data and the calculated IP values with a gas phase IP measurement. The photoelectron spectrum of BDTA, as obtained by vaporization of the radical dimer, is shown in Figure 6. The values for the vertical IP, along with assignments based on Koopmans' estimates (UHF/6-31g**//UHF/cep-31g**)[30] for the first four bands, are listed in Table 4. Figure 1 provides a simplified orbital energy level diagram for the π-levels of BDTA. As expected, and in accord with our previous UPS studies of dithiadiazolyls and thiatriazinyls,[23] the spectrum is characterized by a single low-energy band corresponding to ionization from

(30) Other basis sets showed little variation in the calculated IP values.

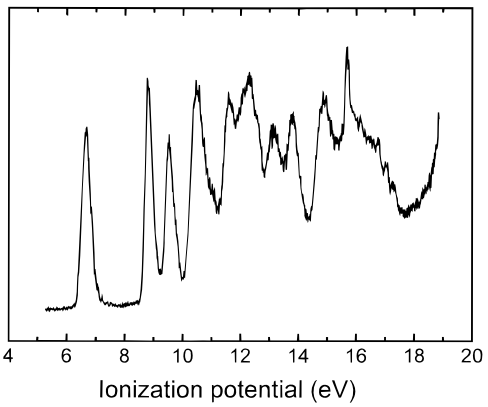

Figure 6. HeI photoelectron spectrum of BDTA, as obtained from the vapor above the dimer at 60 °C.

Table 4. Experimental Adiabatic and Vertical and Predicted[a] Koopmans' IP Values (eV) for BDTA

orbital	$4b_1$	$2a_2$	$3b_1$	$1a_2$
adiabatic IP[b]	6.3	8.5	9.2	10.0
vertical IP[c]	6.66	8.79	9.51	10.46
Koopmans' IP	7.11	8.61	10.05	11.03

[a] The basis set is UHF/6-31g**//UHF/cep-31g**; Koopmans' IP values are scaled by 0.92. [b] The first two adiabatic IP values are ±0.1 eV, while the last two are ±0.2 eV. [c] All vertical IP values are ±0.05 eV.

the $4b_1$ SOMO radical to the closed shell cation. Other, higher energy ionization events will give rise to both singlet and triplet cations, but there is no discernible splitting in any of the higher energy processes. The second, third, and fourth IP values of BDTA are well separated and can thus be easily assigned to the $2a_2$, $3b_1$, and $1a_2$ orbitals illustrated in Figure 1. Below the 10 eV level, the spectrum is considerably more complex. Three σ-levels (two a_1 and one b_2) are predicted in the region of 12−14 eV, and the deepest π-orbital ($1a_1$) is expected near 14 eV. The rich pattern observed in the 12−15 eV region can be attributed collectively to these ionizations, but we refrain from any individual assignments.

Within the context of molecular conductor design, the above CV and UPS data, coupled with the *ab initio* predictions of IP, and EA values summarized in Table 1, provide valuable insight into the potential of 1,3,2-dithiazolyls in general and BBDTA in particular. As predicted by the *ab initio* calculations and as observed experimentally for BDTA, the first vertical IP of BDTA is considerably lower than those found for 1,2,3,5-dithiadiazolyls,[23] comparable to that observed for a strong closed shell donor such as tetrathiafulvalene (TTF, **15**, IP = 6.70−6.92 eV).[31,32] The solution oxidation potentials provide similar

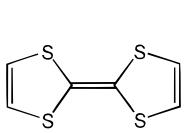

15

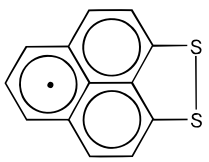

16

conclusions; both BDTA and BBDTA are powerful electron donors, significantly more so than 1,2,3,5-dithiadiazolyls **1**[33]

(31) (a) Berlinsky, A. J.; Carolan, J. F.; Weiler, L. *Can. J. Chem.* **1974**, *52*, 3373. (b) Kobayashi, T.; Yoshida, Z.; Awaji, H.; Kawase, T.; Yoneda, H. *Bull. Chem. Soc. Jpn.* **1984**, *56*, 2591.

(32) Lichtenberger, D. L.; Johnston, R. L.; Hinkelmann, K.; Suzuki, T.; Wudl, F. *J. Am. Chem. Soc.* **1990**, *112*, 3302.

(33) Boeré, R. T.; Moock, K. *J. Am. Chem. Soc.* **1995**, *117*, 4755.

Table 5. Redox and E_{cell} potentials (Volts *vs* SCE) for 1,3,2-Dithiazolyls are Related Compounds[a]

compound	$E_{1/2}$(ox)	$E_{1/2}$(red)	E_{cell}
1 (R = H)[b]	0.65	−0.83	−1.48
BDTA, **5**	0.15	−1.2[c]	−1.32[d]
BBDTA, **6**	0.16, 0.74	−1.3,[c] −1.8[c]	−1.42[d]
TTF^+, $\mathbf{15}^+$ [e]	0.30, 0.66		−0.36[f]
DTPLY, **16**[g]	−0.22	−0.77, −1.55[c]	−0.55

[a] All cell potentials are from solutions in CH_3CN, reference SCE. [b] Potentials from ref 33. [c] Irreversible. [d] This value is taken as the difference in the cathodic peak potentials, since the reduction wave is highly irreversible. [e] Potentials from ref 32. [f] For the reaction 2 TTF^+ = TTF + TTF^{2+}. [g] Potentials from ref 35.

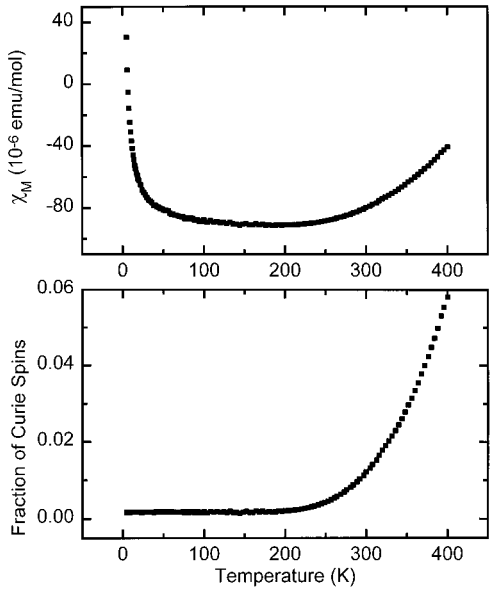

Figure 7. Magnetic susceptibility of polycrystalline BBDTA (above) and fraction of Curie spins (below) as a function of temperature.

and again comparable to TTF,[32,34] although not as strong as the neutral dithiophenalenyl radical (DTPLY, **16**).[35] The E_{cell} data ($E_{cell} = E_{1/2}$(red) + $E_{1/2}$(ox)) provided in Table 5 complement the calculated gas phase disproportionation energies (IP − EA) cited in Table 1. Both sets of data (gas phase and solution) suggest that derivatives based on the 1,3,2-dithiazolyl system should exhibit a reduced barrier to charge transport in the solid state and therefore be superior to 1,2,3,5-dithiadiazolyl derivatives, although both systems exhibit E_{cell} values that are notably higher than either TTF^+ or DTPLY.

Magnetic Susceptibility and Conductivity. The results of variable temperature magnetic susceptibility measurements on polycrystalline BBDTA are shown in Figure 7. In the solid state the material is essentially diamagnetic at low temperatures, with a measured diamagnetism of -95×10^{-6} emu mol^{-1} and a residual spin concentration of 0.17%. Above 250 K, slight paramagnetism occurs, and this increases slowly but steadily to 400 K (the high-temperature limit of the experiment). Figure 7 also illustrates a plot of the fraction of free Curie spins as a function of temperature. Field sweeps did not provide any indication of non-Curie behavior (*e.g.*, ferromagnetism) down to 5 K, the low-temperature limit of the experiment.

Variable temperature single-crystal conductivity measurements on BBDTA have been performed over the temperature range of 250−400 K. A log plot of the conductivity as a function of inverse temperature (Figure 8) shows an excellent linear correlation. On this basis, and if the material is treated as an intrinsic semiconductor, analysis of the data below 300 K leads to a estimated band gap of 0.22 eV.

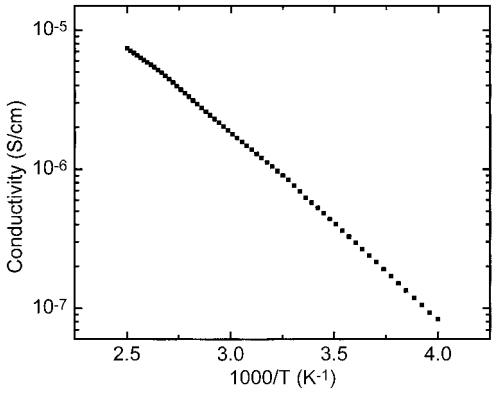

Figure 8. Log plot f conductivity of BBDTA as a function of inverse temperature.

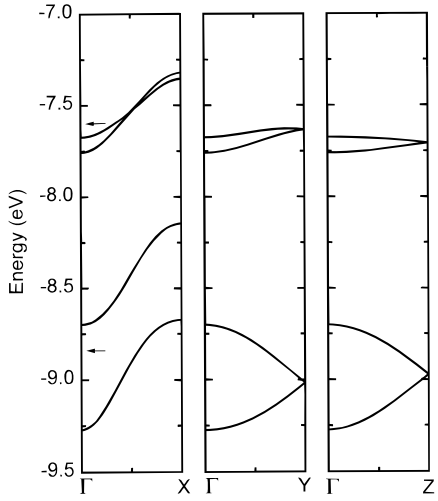

Figure 9. Crystal orbital dispersion of BBDTA along the three principal directions of reciprocal space. The extended Hückel eigenvalues of the b_{1u} and b_{3g} orbitals in isolated BBDTA are indicated by arrows.

Band Calculations. In our previous studies of molecular solids, notably dithiadiazolyls and their selenium counterparts, we have attempted to relate solid state structure to transport properties by means of extended Hückel band structure calculations. Given the diradical electronic structure of BBDTA and the unassociated nature of its solid state structure, its diamagnetism in the solid state is, at first sight, surprising. However, the transport properties of the solid are readily accounted for in terms of the band description of its electronic structure.

The important features of the band structure of BBDTA, namely the width and separation of the valence and conduction bands, can be understood in molecular terms with reference to the two SOMO combinations b_{1u} and b_{3g} described earlier (Figure 2). At the extended Hückel level, these orbitals are well separated in a single molecule of BBDTA; the in-phase combination b_{1u}, in which electron density is spread onto the central carbons of the benzene ring, lies 1.2 eV below the out-of-phase combination b_{3g}. There are two molecules per unit cell in BBDTA, and accordingly, there are crystal orbitals corresponding to two combinations (+ and −) of both of the b_{1u} and b_{3g} molecular orbitals. The dispersion of these four crystal orbital combinations are illustrated in Figure 9 along the three principal directions of reciprocal space. The valence

(34) Bard, A. J.; Faulkner, L. R. In *Electrochemical Methods*; J. Wiley and Sons: New York, 1980.
(35) Haddon, R. C.; Wudl, F.; Kaplan, M. L.; Marshall, J. H.; Cais, R. E.; Bramwell, F. B. *J. Am. Chem. Soc.* **1978**, *100*, 7629.

band arises from the b_{1u} (+ and −) orbitals, while the conduction band is based on the b_{3g} (+ and −) set.

Given the near orthogonality of the unit cell vectors, the magnitude of dispersion can be related with reasonable accuracy to orbital interactions in real space. Within this context several features deserve comment. First, orbital dispersion is larger, in all directions, in the valence band. This can be attributed to the more delocalized nature of the b_{1u} molecular orbital, which spans the benzene ring and thereby affords more effective intermolecular overlap (primarily S−C) between two neighboring BBDTA molecules. Second, dispersion of the valence band is greatest along the stacking direction *a** (*ca*. 1.0 eV), as expected from the slipped stack arrangement shown in Figure 3B. However, dispersion along *b** and *c** is also substantial (*ca*. 0.6 eV), so that in the valence band BBDTA presents a remarkably strong and isotropic electronic structure, comparable to and perhaps even more highly developed than that found in other molecular materials, *e.g.*, dithiadiazolyls such as the benzene-bridged diradical **3**[5a,36] and oligothiophenes such as α-6T.[37]

In all three directions, dispersion of the conduction band orbitals mirrors, although less dramatically, the behavior of the valence band. But, as is readily apparent from Figure 9, the combined dispersion of the valence and conduction bands is insufficient to close the band gap completely. From these calculations the material is thus predicted to be a diamagnetic semiconductor, with an indirect band gap of slightly less than 0.4 eV, a value satisfying close to that derived experimentally from the conductivity measurements.

Summary and Conclusions

In our search for conductive materials based on neutral π-radicals we have studied a wide range of dithiadiazolyl and diselenadiazolyl derivatives. The results described here on the dithiazolyl derivatives BDTA and BBDTA suggest that these systems hold potential advantages to those previously studied. In particular their relatively low ionization/oxidation potentials augur well for a lower Coulombic barrier to charge transfer. The results of *ab initio* calculations substantiate this conclusion and reveal the importance of increasing electron delocalization in BDTA and BBDTA (an option not available in dithiadiazolyls) in decreasing the magnitude of the disproportionation energy (IP − EA). The calculations also indicate minimal exchange interaction between the two radical centers in BBDTA (gas phase), with the triplet state lying slightly (*ca*. 0.5 kcal/mol) lower than the singlet.

In the solid state, BBDTA does not dimerize. The absence of S···S dimerization in the solid state structure of BBDTA allows for more delocalized and isotropic interactions. Intermolecular orbital overlap along and across the slipped stack structure is sufficiently strong to generate a closed shell, diamagnetic electronic structure with a small band gap and a relatively high conductivity for a single-component molecular material.

The present results thus provide a strong impetus for the pursuit of molecular materials based on the 1,3,2-dithiazolyl building block. Variations on both BDTA and BBDTA are currently under investigation.

Experimental Section

Starting Materials and General Procedures. Benzene-1,2,4,5-tetrathiol[38] and benzo-1,3,2-dithiazolyl[13] (BDTA) were prepared according to the literature methods. Triphenylantimony (Aldrich), bis(triphenylphosphine)iminium chloride (Aldrich), nitrosyl hexafluoroantimonate (Strem), and chlorine (Matheson) were all obtained commercially and used as received. Trimethylsilyl azide (Aldrich) was also obtained commercially, but redistilled before use. The solvents (CH_2Cl_2, CH_3CN, CCl_4) were all dried by distillation from P_2O_5 before use. All reactions were performed under an atmosphere of argon. Fractional sublimations of BBDTA were performed in an ATS series 3210 three-zone tube furnace linked to a series 1400 temperature control system. Elemental analyses were performed by MHW Laboratories, Phoenix, AZ 85018. Infrared spectra were recorded (at 2 cm^{-1} resolution on nujol mulls with KBr plates) on a Nicolet 20SX/C infrared spectrometer. Mass spectra (EI, 70 EV) were recorded on a Kratos MS890 mass spectrometer. X-band ESR spectra were recorded on a Varian E-109 spectrometer with DPPH as a field marker. ^1H NMR spectra were recorded on Varian 200 MHz NMR spectrometer. UV-vis spectra were recorded on a Perkin-Elmer Lambda 6 spectrophotometer.

Preparation of Benzene-1,2,4,5-tetra(sulfenyl chloride). Benzene-1,2,4,5-tetrathiol (5.0 g, 24 mmol) was dissolved in 125 mL of carbon tetrachloride, and the solution was cooled in an ice bath. Chlorine gas was then bubbled slowly through the solution. The initially formed yellow precipitate eventually dissolved to yield, after effervescence of HCl gas (20−30 min), an orange solution and an orange precipitate. The solution was then heated briefly to drive off residual HCl and excess Cl_2 and to redissolve the orange precipitate. The solution was cooled to −15 °C overnight. Filtration afforded 5.86 g (17 mmol, 71%) of benzene-1,2,4,5-tetra(sulfenyl chloride)[16,17] as orange needles: mp 98−101 °C; ^1H NMR ($CDCl_3$, δ) 7.91; IR (2000−400 cm^{-1}) 1551(m), 1531(s), 1502(m), 1411(m), 1316(w), 1240(w), 1118(s), 898(m), 853(s), 533(s), 487(s).

Preparation of Benzenebis(dithiazolylium hexafluoroantimonate), [BBDTA][SbF_6]$_2$. Benzene-1,2,4,5-tetra(sulfenyl chloride) (2.83 g, 8.22 mmol) was dissolved in 250 mL of freshly distilled CH_2Cl_2 in a 500 mL flask fitted with an argon inlet and a dropping funnel. A solution of trimethylsilyl azide (1.90 g, 16.5 mmol) in 20 mL of CH_2Cl_2 was then added dropwise. The orange solution darkened quickly, and after 16 h, a heavy red/maroon precipitate of [BBDTA]Cl_2 had formed. The crude dichloride was filtered, washed with two portions of CH_2Cl_2, and dried *in vacuo*: IR (4000−400 cm^{-1}) 3013(vw), 1081(w), 1044(w), 924(w), 775(w), 639(vw), 539(vw).[39] This material was slurried in CH_3CN and treated with solid $NOSbF_6$ (4.50 g, 16.9 mmol). After 4 h, the resulting red solution was concentrated to *ca*. 10 mL and 100 mL of chlorobenzene was added to precipitate benzenebis(dithiazolylium hexafluoroantimonate) [BBDTA][SbF_6]$_2$ as a yellow/orange microcrystalline powder (4.75 g, 6.77 mmol, 82%). Recrystallization from 25 mL/40 mL CH_3CN/chlorobenzene afforded 2.65 g (3.78 mmol, 46%) of bright yellow flakes: mp (dec) > 250 °C; IR (4000−400 cm^{-1}) 3086(w), 1351(w), 1326(vw), 1101(vw), 1088(vw), 1056(w), 972(w), 878(w), 781(w), 666(s, br), 655(s, br), 559(w). Anal. Calcd for $C_6H_2N_2S_4Sb_2F_{12}$: C, 10.27; H, 0.29; N, 3.99. Found: C, 10.64; H, 0.19; N, 4.01.

Preparation of Benzo-1,2:4,5-bis(1,3,2-dithiazolyl), BBDTA. A solution of [BBDTA][SbF_6]$_2$ (2.35 g, 3.35 mmol) in 20 mL of CH_3CN was added dropwise to a stirred solution of PPNCl (4.09 g, 7.13 mmol) and Ph_3Sb (1.25 g, 3.54 mmol) in 150 mL of CH_3CN, and the generated black slurry was stirred overnight. The intense blue solution was then filtered to afford a black precipitate, which was washed with a small portions of CH_3CN and dried *in vacuo* to yield crude BBDTA (0.625 g, 2.72 mmol). The product was purified by fractional sublimation *in vacuo* (120−80 °C/10^{-3} Torr) in a gradient tube sublimer to afford lustrous copper blocks of BBDTA (0.250 g, 1.09 mmol, 33%): mp

(36) Cordes, A. W.; Haddon, R. C.; MacKinnon, C. D.; Oakley, R. T.; Patenaude, G. W.; Reed, R. W.; Rietveld, T.; Vajda, K. E. *Inorg. Chem.* **1996**, *35*, 7626.

(37) (a) Haddon, R. C.; Siegrist, T.; Fleming, R. M.; Bridenbaugh, P. M.; Laudise, R. A. *J. Mater. Chem.* **1995**, *5*, 1719. (b) Siegrist, T.; Fleming, R. M.; Haddon, R. C.; Laudise, R. A.; Lovinger, A. J.; Katz, H. E.; Bridenbaugh, P.; Davis, D. D. *J. Mater. Res.* **1995**, *10*, 2170.

(38) Cox, D.; Wellman, D. E.; Wudl, F. *J. Org. Chem.* **1985**, *50*, 2395.

(39) Our infrared spectrum of [BBDTA]Cl_2 differs significantly from that reported by previous workers (refs 16 and 17). The success of this reaction is highly dependent on the purity of the starting tetra(sulfenyl chloride).

259−60 °C; IR (4000−400 cm^{-1}) 3084(vw), 1403(w), 1343(vw), 1074-(m), 869(m), 841(s), 696(vs), 650(w), 413(m); MS (*m*/*z*) 230 (M^+, 100); UV-vis (CH_2Cl_2) 571 (1.2×10^4), 315 (6.7×10^3), 269 (1.4×10^4), 241 (1.9×10^4) nm (M^{-1} cm^{-1}). Anal. Calcd for $C_6H_2N_2S_4$: C, 31.29; H, 0.88; N, 12.16. Found: C, 31.36; H, 0.63; N, 12.27.

Cyclic Voltammetry. Cyclic voltammetry was performed on a PAR 273A electrochemical system (EG&G Instruments) with scan rates of 50−100 mV s^{-1} on solutions of the diradical (0.1 M tetra-*n*-butylammonium hexafluorophosphate) in acetonitrile. Potentials were scanned from −2.5 to 1.5 V with respect to the quasi-reference electrode in a single compartment cell fitted with platinum electrodes and referenced to the ferrocenium/ferrocene couple at 0.38 V *vs* SCE.[40]

UV Photoelectron Spectrum. The PE spectrum of BDTA (**5**) was recorded on a photoelectron spectrometer constructed using components supplied by Comstock, Inc., Oak Ridge, TN. These included a mean 4 in. hemispherical analyzer in conjunction with chevronned 50 mm hemispherical plates acting as a position-sensitive detector. Readout was by means of a resistive anode. This instrument, described elsewhere,[41] provides an energy bite of 20% of the transmission energy. The spectrum shown in Figure 6 was recorded with a transmission energy of 20 eV, giving a resolution of 60 meV and an energy bite of 4 eV. Six overlapping windows of data were collected, normalized, and assembled using Lotus 1-2-3. The sample was introduced as its dimer, from which the radical was generated by gentle heating (50 °C). A total of 30 000 scans were measured. The spectrum was calibrated using Ar and acetone.

Ab Initio Molecular Orbital Calculations. All calculations were run on Silicon Graphics workstations. Initial calculations used the Gamess95 program[42] with the effective core potential cep-31G** approach of Stevens, Basch, and Krauss.[43] The d-type polarization functions were the same as previously used,[7] with coefficients of 0.75 (C), 0.80 (N), and 0.532 (S). These results included RHF, UHF, ROHF, GVB-PP, and single-point CI. Later results were obtained from the Gaussian92/DFT, revision G.2, suite of programs[44] using the same cep basis set, but with the exponents of the polarization and diffuse functions taken from Gaussian92. The geometry optimizations used the analytical gradient methods employed in the Gamess95 program, with all minima verified by vibrational frequency analysis. $\langle S^2 \rangle$ values for the UHF calculations on BBDTA were between 2.0 and 2.6 for the triplet and ranged from 0.8 to 1.7 for the doublets. Despite the significant spin contamination for the doublet species, the energetic results were comparable (within 0.3 eV) between the UHF and ROHF methods.

Table 6. Crystal Data for BBDTA

formula	$S_4N_2C_6H_2$
fw	230.33
a, Å	4.144(2)
b, Å	9.0344(13)
c, Å	10.7424(16)
β, deg	91.11(3)
V, Å^3	402.1(2)
space group	$P2_1/c$
Z	2
temp, K	293
μ, mm^{-1}	1.07
data with $I > 2.5\sigma(I)$	613
parameters refined	55
$R(F)$, $R_w(F)$	0.028, 0.048

[a] $R = [\sum||F_o| - |F_c||]/[\sum|F_o|]$; $R_w = \{[\sum w||F_o| - |F_c||^2]/[\sum(w|F_o|^2)]\}^{1/2}$.

Band Structure Calculations. The band structure calculations were performed on a Pentium 166 personal computer with the EHMACC suite of programs[45] using the parameters discussed previously.[5a,46] The off-diagonal elements of the Hamiltonian matrix were calculated with the standard weighting formula.[47]

X-ray Measurements. All X-ray data were collected on an ENRAF-Nonius CAD-4 diffactometer with monochromated Mo Kα radiation. Crystals of BBDTA were mounted on a glass fiber with silicone. Data were collected using a $\theta/2\theta$ technique. The structures were solved using direct methods and refined by full-matrix least squares which minimized $\sum w(\Delta F)^2$. A summary of crystallographic data is provided in Table 6.

Magnetic Susceptibility and Conductivity Measurements. The magnetic susceptibility of BBDTA over the temperature range of 5−400 K were measured using a SQUID magnetometer operating at 1 Tesla. Four-point conductivity measurements were performed with a Keithley 236/617 unit; wires were attached with silver epoxy. Given the blocklike morphology of the crystals the correspondence of the measurement to a crystallographic direction is uncertain. The conductivity was, however, isotropic for the two directions measured.

Acknowledgment. We thank the Natural Sciences and Engineering Research Council of Canada, the NSF/EPSCOR program, and the State of Arkansas for financial support. T.M.B. acknowledges the Department of Education for a doctoral fellowship.

Supporting Information Available: Tables of optimized *ab initio* geometries for the different oxidation states of DTA, BDTA, and BBDTA and tables of crystal data, structure solution, and refinement, bond lengths and angles, and anisotropic thermal parameters for BBDTA (6 pages). See any current masthead page for ordering and Internet access instructions.

JA9636294

(40) Boeré, R. T.; Moock, K. H.; Parvez, M. *Z. Anorg. Allg. Chem.* **1994**, *620*, 1589.
(41) de Laat, R. H. M.Sc. Thesis, University of Guelph, 1993.
(42) Schmidt, M. W.; Baldridge, K. K.; Boatz, J. A.; Elbert, S. T.; Gordon, M. S.; Jensen, J. J.; Koseki, S.; Matsunaga, N.; Nguyen, K. A.; Su, S.; Windus, T. L.; Dupuis, M.; Montgomery, J. A. *J. Comput. Chem.* **1993**, *14*, 1347.
(43) (a) Stevens, W. J.; Basch, H.; Krauss, M. *J. Chem. Phys.* **1984**, *81*, 6026. (b) Stevens, W. J.; Basch, H.; Krauss, M.; Jasien, P. *Can. J. Chem.* **1992**, *70*, 612. (c) Cundari, T. R.; Stevens, W. J. *J. Chem. Phys.* **1993**, *98*, 5555.
(44) Frisch, M. J.; Trucks, G. W.; Schlegel, H. B.; Gill, P. M. W.; Johnson, B. G.; Wong, R.; Foresman, J. B.; Robb, M. A.; Head-Gordon, M.; Replogle, E. S.; Gomperts, R.; Andres, J. L.; Ragavachari, K.; Binkley, J. S.; Gonzalez, C.; Martin, R. L.; Fox, D. J.; Defrees, D. J.; Baker, J.; Stewart, J. J. P.; Pople, J. A. *Gaussian92/DFT*, Revision G.2; Gaussian, Inc.: Pittsburgh, PA, 1993.
(45) EHMACC, Quantum Chemistry Program Exchange, program number 571.
(46) Basch, H.; Viste, A.; Gray, H. B. *Theor. Chim. Acta* **1965**, *3*, 458.
(47) Ammeter, J. H.; Burghi, H. B.; Thibeault, J. C.; Hoffmann, R. *J. Am. Chem. Soc.* **1978**, *100*, 3686.